Carbonization Mechanism of Tetrapropylammonium-hydroxide in Channels of $AlPO_4$-5 Single Crystals

Jian Pang Zhai,[†,§] Zi Kang Tang,*[,†] Zhao Ming Li,[†] Irene Ling Li,[‡] Fu Yi Jiang,[†] Ping Sheng,[†] and Xijun Hu[§]

Department of Physics, Hong Kong University of Science and Technology, Department of Chemical Engineering, Hong Kong University of Science and Technology, Clear Water Bay, Kowloon, Hong Kong, China, and School of Engineering and Technology, Shenzhen University, Shenzhen, China

Received December 4, 2005. Revised Manuscript Received January 19, 2006

We studied the carbonization mechanism of tetrapropylammonium-hydroxide (TPAOH) carbon precursors in the channels of $AlPO_4$-5 crystal, with the aim of producing higher-density and better-quality 4 Å carbon nanotubes. The conversion process of TPAOH was investigated by using a combination of Fourier transform infrared (FTIR) spectra, mass spectrometry, and micro-Raman spectroscopy under various pyrolysis temperatures. During the pyrolysis process, the TPAOH molecules decomposed into lighter amines with the abstraction of propylene, with the stepwise formation of tripropylamine, dipropylamine, and *n*-propylamine. This leads to the formation of 0.4 nm single-walled carbon nanotubes (SWNTs) at about 723 K. The SWNTs density was found to be higher than that resulting from the carbon precursor of tripropylamine (TPA), because of the larger number of carbon atoms in the unit cell. Thermogravimetry (TG) measurements also indicated a higher loading density (in $AlPO_4$-5 crystals) for the TPAOH carbon precursors.

1. Introduction

The discovery of carbon nanotubes[1] has propelled a tremendous wave in the study of their novel properties and potential applications.[2] Because of carbon nanotubes' 1D character, the control of their alignment and diameter has been a crucial issue for both applications and experiments aimed at clarifying their physical characteristics. In our earlier work, we have fabricated ultrathin, single-walled carbon nanotubes (SWNTs) with a diameter as small as 0.4 nm in the channels of $AlPO_4$-5 zeolite (structure code AFI) crystals.[3−5] These perfectly aligned 0.4 nm SWNTs provide a platform on which the experimental and theoretical studies can be carried out on the quasi-one-dimensional (1D) material system.[6−9]

The ultrathin SWNTs were generated by the pyrolysis of TPA ($(CH_3CH_2CH_2)_3N$) hydrocarbon molecules, incorporated in the channels as an organic template during the synthesis of the $AlPO_4$-5 crystal. As the $AlPO_4$-5 framework is largely inert, the adsorption of the guest molecules to the channel wall is relatively weak. As a result, a significant amount of hydrocarbon precursor molecules can escape from the channels during the pyrolysis. The remaining carbon atoms are insufficient in number to form continuous carbon nanotubes. The density of the SWNTs in the $AlPO_4$-5 matrix is thus fairly low. As the nanotubes are most likely rich in structural defects and low in filling factor, the electrical conduction is poor, as evidenced by the 1D hopping conduction along the nanotubes[9] and diffuse X-ray scattering.[10]

The number of carbon atoms in the precursor molecule is a crucial factor in forming better-quality SWNTs. As the structural quality of the SWNT−$AlPO_4$-5 samples would greatly affect the physical properties of the nanotube−zeolite composite, it is the aim of this work to produce better-quality SWNTs with a high filling factor.

To increase the density of carbon atoms in the AFI channels, we can employ two approaches. The first is to generate a negatively charged framework, with Brønsted acid sites, by replacing P^{5+} using Si^{4+}, or replacing Al^{3+} using divalent metallic cations (Me^{2+}) such as Mn^{2+}, Mg^{2+}, and Co^{2+} in the $AlPO_4$-5 crystal frames. The introduced metallic cation sites would not only enhance the adsorption force of the channel walls to the guest molecules but can also play an important catalytic role in paralyzing the carbon precursor molecules.[11,12] The second approach is the in situ synthesis

* To whom correspondence should be addressed. E-mail: phzktang@ust.hk.
† Department of Physics, Hong Kong University of Science and Technology.
§ Department of Chemical Engineering, Hong Kong University of Science and Technology.
‡ Shenzhen University.

(1) Iijima, S. *Nature* **1991**, *354*, 56.
(2) Dresselhaus, M. S.; Dresselhaus, G. *Carbon Nanotubes: Synthesis, Structure, Properties and Applications*; Springer: Berlin, 2001.
(3) Tang, Z. K.; Sun, H. D.; Wang, J.; Chen, J.; Li, G. *Appl. Phys. Lett.* **1998**, *73*, 2287.
(4) Sun, H. D.; Tang, Z. K.; Chen, J.; Li, G. *Appl. Phys. A.* **1999**, *69*, 381.
(5) Wang, N.; Tang, Z. K.; Li, G. D.; Chen, J. S. *Nature* **2000**, *408*, 50.
(6) Li, Z. M.; Tang, Z. K.; Liu, H. J.; Wang, N.; Chan, C. T.; Saito, R.; Okada, S.; Li, G. D.; Chen, J. S. *Phys. Rev. Lett.* **2001**, *87*, 127401.
(7) Sun, H. D.; Tang, Z. K.; Chen, J.; Li, G. *Solid State Commun.* **1999**, *109*, 365.
(8) Li, I. L.; Tang, Z. K. *Appl. Phys. Lett.* **2003**, *82*, 1467.
(9) Tang, Z. K.; Zhang, L.; Wang, N.; Zhang, X. X.; Wen, G. H.; Li, G. D.; Wang, J. N.; Chan, C. T.; Sheng, P. *Science* **2001**, *292*, 2462.
(10) Launois, P.; Moret, R.; Le Bolloc'h, D.; Albouy, P. A.; Tang, Z. K.; Li, G.; Chen, J. *Solid State Commun.* **2000**, *116*, 99.
(11) Li, Z. M.; Zhai, J. P.; Liu, H. J.; Li, I. L.; Chan, C. T.; Sheng, P.; Tang, Z. K. *Appl. Phys. Lett.* **2004**, *85*, 1253.

10.1021/cm0526821 CCC: $33.50
Published on Web 02/14/2006

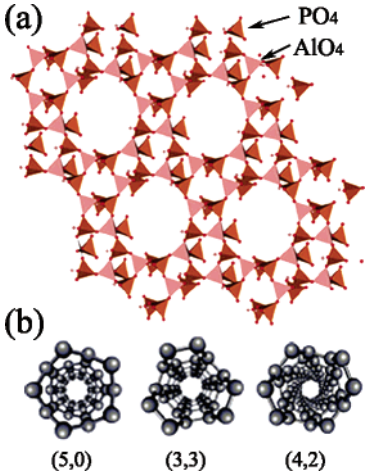

Figure 1. (a) Framework structure of an $AlPO_4$-5 crystal, viewed along the [001] direction. (b) Three possible structures for the 0.4 nm SWNTs inside the channels: (5,0), (4,2), and (3,3).

of $AlPO_4$-5 crystals with organic templates that have a richer carbon content. An organic precursor with a higher carbon content should be more facile to the formation of carbon nanotubes and should thereby improve the SWNT filling density. This work aims to study the latter approach and to examine in more detail the mechanism of carbonization for one of the organic precursors, so as to better optimize the pyrolysis process.

We show that the filling density of the SWNTs can indeed be significantly improved by using precursors with a carbon content richer than that of the TPA, and the tetrapropylammonium-hydroxide ($(CH_3CH_2CH_2)_4NOH$ TPAOH) is found to be the best. In particular, the carbonization process of the TPAOH molecules (in the channels of $AlPO_4$-5 crystals) was observed to consist of stepped decomposition into lighter amines through the sequential abstraction of propylene in the temperature range 523−723 K. Micro-Raman measurements show the 0.4 nm nanotubes to be formed at about 723 K.

2. Experimental Section

The $AlPO_4$-5 framework is composed of alternating tetrahedral $(AlO_4)^-$ and $(PO_4)^+$, which form parallel open channels and are packed in the hexagonal structure with space group *P*6*cc*. The inner diameter of the 12-ring channel is 0.73 nm. Organic template molecules in the channels were oriented in a head−tail manner along the *c* axis.[13] Its framework structure viewed along the [001] (*c* axis) direction is shown in Figure 1a. A pure $AlPO_4$-5 crystal is optically transparent from ultraviolet to near-infrared, a good insulator, and thermally stable up to 1173 K. Hence nanomaterials accommodated in its channels can be probed both optically and electrically.[14,15] $AlPO_4$-5 single crystals were synthesized using a hydrothermal process with gel compositions of 1.0:1.0:1.2:0.8:400 Al_2O_3:P_2O_5:*R*:HF:H_2O, where *R* is the carbon precursor template. Aluminum tri-isopropoxide ($(i\text{PrO})_3Al$) and phosphoric acid (H_3PO_4, 85 wt %) were used as the aluminum and phosphorus sources, respectively. One of the following carbon precursor molecules was employed as the template for the $AlPO_4$-5 crystal growth: triethylamine ($(CH_3CH_2)_3N$, TEA), TPA ($(CH_3CH_2CH_2)_3N$), TPAOH ($(CH_3CH_2CH_2)_4NOH$), and tetrabutylammonium hydroxide ($(CH_3CH_2CH_2CH_2)_4NOH$, TBAOH). The typical synthesis procedure is as follows: (1) the aluminum source is first dissolved in distilled water, followed by the dropwise addition of phosphoric acid with stirring; (2) the organic template is added to the viscous aluminophosphate gel; (3) the aqueous HF solution is slowly added to the homogeneous slurry; (4) the gel formed from the reaction mixture is sealed in a Teflon-lined stainless autoclave and heated to 448 K under autogenous pressure for 24 h; and (5) finally, the solid products are filtered, washed with distilled water, and dried at 353 K.

The framework of the $AlPO_4$-5 crystals is built around the organic species TPA^+, which occurs in the solid as an ionic pair TPA^+OH^- or TPA^+F^-, in accordance with the synthesis medium.[13,16] SWNTs are produced by pyrolyzing the carbon precursor templates in rising temperature steps. The detailed process was described in ref 7. The diameter of the SWNTs generated in the AFI channels is 0.4 nm.[5,10,17] Figure 1b schematically shows three possible tube structures viewed along the tube direction. Here, we repeat the same procedure to fabricate the 0.4 nm SWNTs by pyrolyzing different carbon precursor molecules (TEA, TPA, TPAOH, and TBAOH) directly in a vacuum of 10^{-3} mbar at temperatures up to 853 K.

Raman spectra of the SWNT-containing $AlPO_4$-5 single crystals were measured at room temperature by using a Jobin Yvon-T64000 micro-Raman spectrometer, with the 514.5 nm line of an Ar ion laser as the excitation. The equipped CCD detector is cooled by liquid nitrogen. The incident laser light was polarized parallel to the nanotube axis. The thermal adsorption/desorption process of the different carbon precursors in the channels was recorded using a thermal analysis apparatus (STA 449C Jupiter). The mass resolution of the equipment is 0.1 μg. Fourier transform infrared (FTIR) spectra were recorded using a FTIR spectrometer (Bio-Rad FTS 6000) for in situ monitoring the pyrolysis process of carbon precursor TPAOH (in the channels) at various temperatures. A programmable furnace was interfaced with a mass spectrometer in order to identify the decomposition products escaping from the $AlPO_4$-5 channels. The volatiles that evolved from the TPAOH were measured by an ABB mass spectrometer.

3. Results and Discussion

The as-grown $AlPO_4$-5 crystals have a typical size of 500 μm × 50 μm × 50 μm. All crystals are regular hexagonal cylinders in shape and have a good morphology (see Figure 2b, left]. The crystallinity of as-synthesized samples was checked by powder X-ray diffraction (Philips PW1830 diffractometer). The $AlPO_4$-5 crystals with various organic templates show the same X-ray diffraction pattern as the pure AFI crystal.

3.1. Effect of Different Carbon Precursors on the Formation of SWNTs. To see how the carbon sources affect the filling factor of carbon nanotubes, we used four carbon precursors, which have a different number of carbon atoms per molecule, in the synthesis of SWNTs inside the AFI channels. They are TEA, TPA, TPAOH, and TBAOH, which contain 6, 9, 12, and 16 carbon atoms per unit cell, respectively. Their molecular structures are shown in Figure 2a.

(12) Zhai, J. P.; Li, Z. M.; Liu, H. J.; Li, I. L.; Sheng, P.; Hu, X. J.; Tang, Z. K. *Carbon* **2005**, accepted.
(13) Qiu, S.; Pang, W.; Kessler, H.; Guth, J. L. *Zeolite* **1989**, *9*, 440.
(14) Li, I. L.; Tang, Z. K. *Appl. Phys. Lett.* **2002**, *80*, 4822.
(15) Li, I. L.; Tang, Z. K.; Xiao, X. D.; Yang, C. L.; Ge, W. K. *Appl. Phys. Lett.* **2003**, *83*, 2438.
(16)] Soulard, M.; Bilger, S.; Kessler, H.; Guth, L. *Zeolites* **1987**, *7*, 463.
(17) Li, Z. M.; Tang, Z. K.; Siu, G. G.; Bozovic, I. *Appl. Phys. Lett.* **2004**, *84*, 4101.

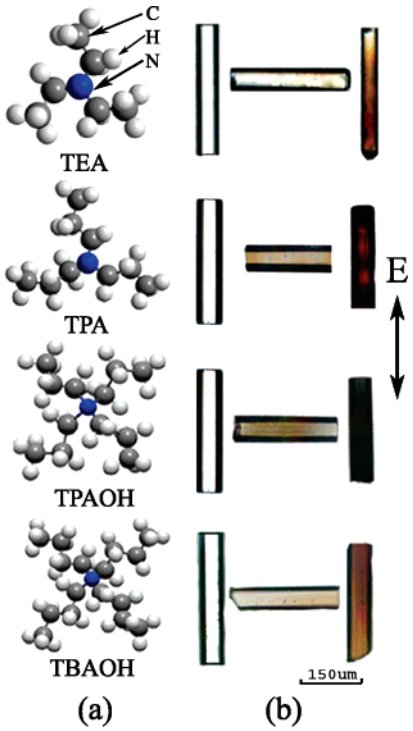

Figure 2. (a) Molecular structures of various organic templates. (b) Microscopic view of the SWNT−$AlPO_4$-5 pyrolyzed in a vacuum of 10^{-3} mbar: $AlPO_4$-5 single crystal without SWNTs (left), images taken under the light polarized perpendicular to the tube direction (middle), and under the light polarized parallel to the tube direction (right).

The $AlPO_4$-5 crystals containing the carbon precursors are transparent in color (see Figure 2b, left). When gradually heated in a vacuum of 10^{-3} mbar up to a temperature of 673 K, the crystals turned homogeneous black with strong optical anisotropy.[6,18,19] From the optical anisotropy and the black color, we can qualitatively estimate the quality of the SWNTs formed in the channels. In the two panels on the middle and right side of Figure 2b, we show optical microscope images of the SWNT−$AlPO_4$-5 single crystals. These images were taken by inserting a polarizer (vertically polarized) in the optical path. For the *E*//*c* configuration, we see that for those samples produced using carbon precursors that contained more carbon atoms (from TEA to TPAOH), the color is darker and more uniform. This indicates that the filling density of the SWNTs is improved. However, for the sample with TBAOH as the carbon precursor, though the number of carbon atoms per molecule is larger than that for all the other precursors, the produced SWNT−AFI crystals show less anisotropy with a relative diluted black color.

A significant difference in the SWNTs formed using different carbon precursors can also be evidenced by the Raman spectra, as shown in Figure 3. Generally, the Raman spectra exhibit three main features: the tangential *G* bands in the high-frequency region (1500−1620 cm^{-1}) due to the bond stretching vibrations; the *D* bands in the intermediate frequency region (1200−1500 cm^{-1}) due to disordered carbons; and the radial breathing mode (RBM) in the low-

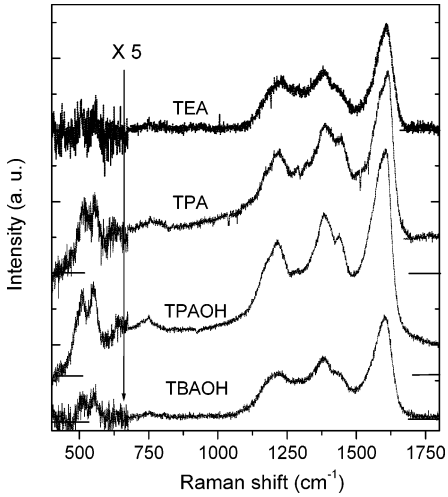

Figure 3. Raman spectra of the SWNTs produced using various carbon precursors.

frequency region (400−600 cm^{-1}) due to tubular vibrations along the radial direction. In particular, the Raman lines at 510 and 550 cm^{-1} shown in Figure 3 are attributed to the A_{1g} RBM of the chiral (4, 2) nanotubes and the zigzag (5, 0) nanotubes, respectively.[17,20] As the RBM vibrations are specific to the tubular structure, we use the relative RBM to *G* band ratio (I_{RBM}:I_G) as a measure of the tubular carbon structure contained in the AFI channels. Larger values of I_{RBM}:I_G imply a higher filling density of the carbon nanotubes. The relative intensities of the RBM bands at 510 and 550 cm^{-1} are obviously enhanced with an increase in the carbon number per precursor molecule (from TEA to TPAOH). On the other hand, the line width of the *G* band near 1600 cm^{-1} became narrow upon the increase in carbon atoms per molecule (from TPA to TPAOH), indicating that the hydrocarbon molecules are well graphitized in the channels. However, a further increase in the carbon content led to a decrease in the relative RBM intensity when TBAOH was adopted as the carbon precursor. The RBMs of the SWNTs generated from TEA and TBAOH are almost undetectable from the background noise. We thus conclude that TPAOH is superior to both TEA and TPA as the carbon precursor for the growth of 0.4 nm SWNTs.

Figure 4a shows the measured TG curves of the SWNT−$AlPO_4$-5 crystals grown using different carbon precursors. The weight loss in the temperature region from 320 to 400 K is due to the moisture desorption. If it is assumed that all the $AlPO_4$-5 crystals channels are saturated with SWNTs and water, then a larger weight loss of water implies a lower filling density of SWNTs inside the channels. In comparison with that in TEA, TPA, and TBAOH, the weight loss of water in the sample prepared using TPAOH as the carbon precursor (see the inset of Figure 4) is relatively low, indicating a higher filling fraction of SWNTs in this sample.

When studying the effect of carbon precursors on the filling factor of the SWNTs in the channels of $AlPO_4$-5 crystals under the same synthesis conditions, it is important to know the initial loading densities of the respective carbon

(18) Ajiki, H.; Ando, T. *Physica B* **1994**, *201*, 349.
(19) Li, Z. M.; Liu, H. J.; Ye, J. T.; Chan, C. T.; Tang, Z. K. *Appl. Phys. A* **2004**, *78*, 1121.
(20) Jorio, A.; Filho, A. G. S.; Dresselhaus, G.; Dresselhaus, M. S.; Righi, A.; Matinaga, F. M.; Dantas, M. S. S.; Pimenta, M. A.; Filho, J. M.; Li, Z. M.; Tang, Z. K.; Saito, R. *Chem. Phys. Lett.* **2002**, *351*, 27.

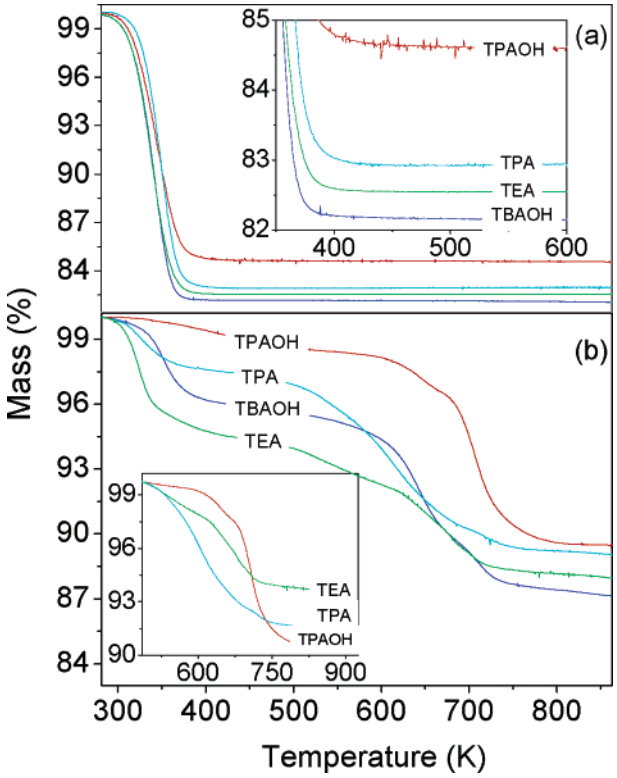

Figure 4. TG curves measured at temperatures ranging from 273 to 873K for: (a) SWNT−$AlPO_4$-5 crystals using various organic templates as carbon precursors, and (b) $AlPO_4$-5 crystals with various organic templates inside the channels.

precursors inside the channels. We have traced the gravimetric change of $AlPO_4$-5 crystals containing various carbon precursors during heating. As shown in Figure 4b, the common TG curve features of $AlPO_4$-5 crystals with different carbon precursors are similar to each other. They exhibit two main features: the weight loss in the region from 320 to 400 K is due to the moisture desorption, and the loss in the region from 483 to 800 K is due to the decomposition of carbon precursors. The signal becomes flattened when the sample is heated to above 800 K, indicating a complete decomposition of hydrocarbon precursors. The channels of an as-grown $AlPO_4$-5 crystal are fully occupied by crystal water as well as hydrocarbon molecules. Thus the weight loss of water is an indicator of the carbon precursor's loading density; more weight loss of water thus indicates a lower loading density of the carbon precursors. Not surprisingly, the weight loss of $AlPO_4$-5 crystals due to the moisture desorption decreases with an increasing initial carbon content in carbon precursors (from TEA to TPAOH). The exception is again TBAOH. This can be due to the fact that the molecular size of TBAOH is so big that the lattice matching between the TBAOH and $AlPO_4$-5 unit cell is not perfect, leading to increased intermolecular space. The mismatch results in an even lower loading density, in comparison with the well-fitted molecules of TAP and TPAOH. The inset to Figure 3b shows the TG curve of TPA. As a reference, we show the corresponding curves of TEA and TPAOH inside the channels of $AlPO_4$-5 crystals. It is seen that the mass loss of carbon precursors increases with an increasing internal carbon content (in carbon precursors), because of the higher loading density. Thus the TPAOH organic template is so far the best carbon precursor for fabricating higher-density SWNTs.

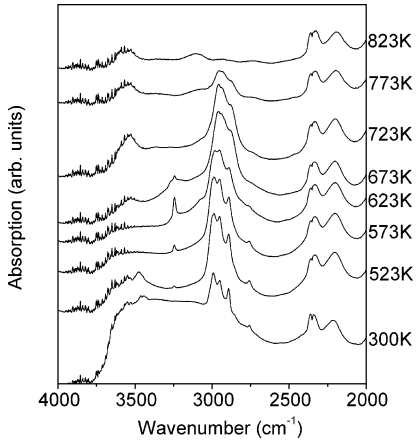

Figure 5. FTIR spectra of $AlPO_4$-5 crystals containing TPAOH, recorded at various temperatures under a nitrogen atmosphere.

3.2. Carbonization Process of TPAOH inside the Channels of the $AlPO_4$-5 Crystal. To study the carbonization process of TPAOH molecules in the $AlPO_4$-5 crystals channels, we pressed 0.5 mg of crystal powder into a tablet and put it on a temperature-controlled holder for in situ FTIR spectral measurement with continuously flowing nitrogen gas. The temperatures was varied from 323 to 823 K. Figure 5 shows the FTIR spectra in the frequency region 2000−4000 cm^{-1}. At room temperature, the spectrum exhibits three main features: the peaks in the region 2000−2600 cm^{-1} can be assigned to the overtones plus their combinations of the Al−O−P vibrations (from the $AlPO_4$-5 crystal framework); the peaks in the region 2600−3400 cm^{-1} are due to the TPAOH molecules; and the peaks in the region 3400−3700 cm^{-1} are attributable to the O−H vibration of the water molecules.[21,22] With increasing temperature, the relative intensity of the O−H band weakens, becoming undetectable above 573 K and implying desorption of water. At this point, the spectrum resembles to some extent that of TPA free molecules.[11] We can thus assume that tetrapropylammonium ion $(CH_3CH_2CH_2)_4N^+$ has been partially converted to $(CH_3CH_2CH_2)_3N$. As evidence, the N−H stretching vibration mode at 3243 cm^{-1} is observed at this temperature. With a further temperature increase to 623 K, the relative intensity of the N−H peak increases, implying that the thermal treatment leads to the formation of dipropylamine [$(CH_3CH_2CH_2)_2NH$] or *n*-propylamine [$(CH_3CH_2CH_2)NH_2$] by the sequential abstraction of propylene from the TPA $(CH_3CH_2CH_2)_3N$ molecules. At even higher temperatures, the N−H vibration signal decreases and completely disappears above 723 K, indicating that the propylene (C_6H_6) is released from the dipropylamine molecules and that the ammonia molecules were desorbed from the channels. In the C−H vibration region, the bands at 2892 and 2950 cm^{-1} became weaker and finally became undetectable above 823 K, indicating that at this temperature, the C−H bonds of C_3H_6, or its smaller oligomers have started to break. Because of its light mass

(21) Sorina, C.; Popescu, S. T.; Russell, F. H. *Phys. Chem. Chem. Phys.* **2001**, *3*, 111.
(22) Schnabel, K. H.; Finger, G.; Kornatowski, J.; Elke L.; Peuker, C.; Pilz, W. *Microporous Mater.* **1997**, *11*, 293.

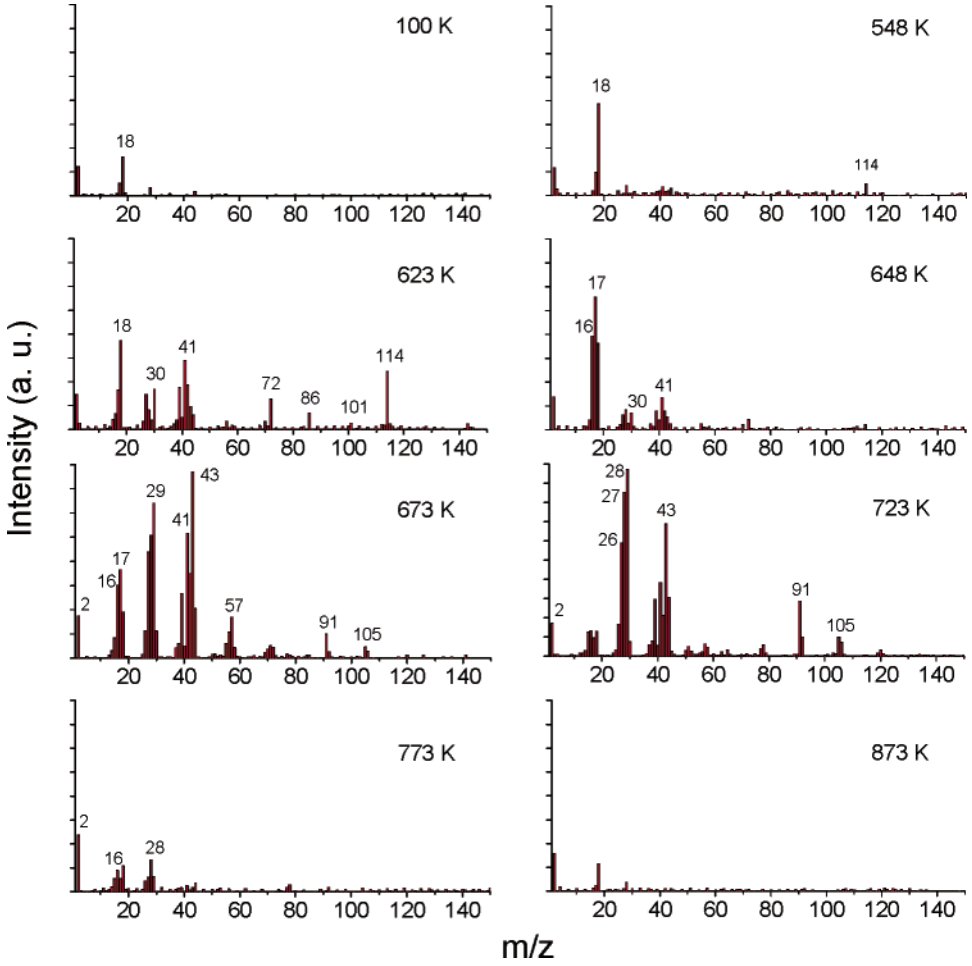

Figure 6. Mass spectra obtained at various points during the thermal pyrolysis of a TPAOH template occluded within $AlPO_4$-5 crystals.

and higher mobility, hydrogen molecules would escape from the channels, whereas carbon atoms are expected to mostly remain.

FTIR spectra can monitor only the decomposition process that happens inside the crystal channel; they cannot identify the gas species that escape from the channels. The use of a mass spectrometer remedied this situation. We used mass spectrometry to monitor the pyrolysis process of TPAOH molecules in a vacuum. The total mass spectra recorded at different temperatures are shown in Figure 6. By elevating the temperature to 548 K, we were able to significantly increase the water signals (m/z = 18 and 17) because of desorption. The presence of new m/z signals at 114, 86, and 72 are attributable to the formation of neutral TPA, and these signals increased when the sample was heated to 623 K. The spectra recorded between 548 and 648 K indicate the decomposition of the TPA template molecules to lower amines and propylene via sequential Hofmann elimination reactions. This is evidenced by the m/z signals at 101, 72, and 30 attributable to dipropylamine and *n*-propylamine; the signals at 42, 41, 39, and 27 attributable to propylene; and the signals at 17 and 16 attributable to ammonia (NH_3). It is worth pointing out that the water signals decreased in the temperature range 548−623 K, whereas that of TPA increased because the occluded tetrapropylammonium fluoride is more stable than the hydroxide, which is comparable to the results of Soulard et al.,[16] who investigated decomposition of tetrapropylammonium ions in MFI-type zeolites by means of thermoanalytical techniques. On heating to 673 K, the iron signals at m/e 91, 92, 105, and 106 were observed. These are characteristic of xylene. The mass spectral data (m/z = 72, 57, 56, 55, 43, 42, 41, 39, 29, and 27) confirmed that 2-methyl-butane (C_5H_{12}) were also produced and suggested that propane and butane may also have been produced. It is possible that a small amount of catalytic activity was responsible for this. The signals of 2-methyl-butane became weaker and finally undetectable when the sample was heated to 773 K, whereas the intensities of H_2 (m/z = 2), C_2H_4 (m/z = 28, 27, and 26) and CH_4 (m/z = 16 and 15) increased. With a further increase in temperature, the intensities of all the above-mentioned signals deceased and finally became negligible when the heating temperature reached 873 K or above. These observations agree well with the earlier report by Parker et al.,[23] who investigated the decomposition of TPAOH in MFI-type zeolites, except TPA was not observed as a volatile product in their study. A similar mechanism has been claimed by Bourgeatlami et al.,[24] who investigated the decomposition of tetraethylammonium ions in the zeolite Beta. A common conclusion is that the template molecules decompose to lower amines and ethylene through sequential Hofmann elimination reactions. By combining the results of

(23) Parker, L. M.; Bibby, D. M.; Patterson, J. E. *Zeolites* **1984**, *4*, 168.
(24) Elodie, B. L.; Francesco, D. R.; Francois, F.; Piere, H. M.; Thiery, D. C. *J. Phys. Chem.* **1992**, *96*, 3807.

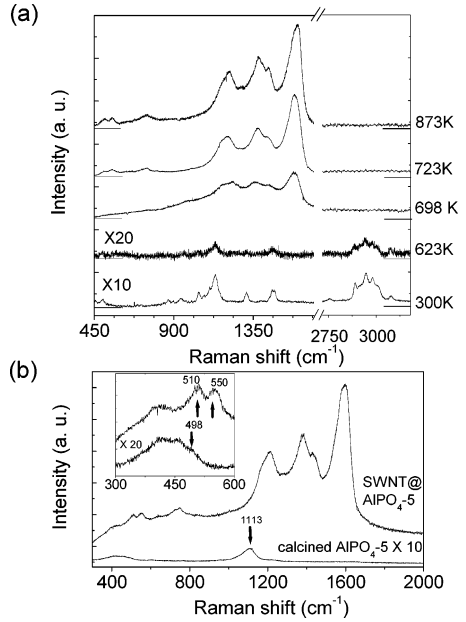

Figure 7. (a) Raman spectra of the $AlPO_4$-5 crystals, measured at different pyrolysis temperatures in a vacuum of 10^{-3} mbar; (b) Raman spectra of 0.4 nm SWNTs formed inside the channels of $AlPO_4$-5 and calcined $AlPO_4$-5 single crystal.

FTIR measurements and mass spectra, we propose the following flowchart for the decomposition process of the TPAOH organic molecules

$$[(CH_3CH_2CH_2)_4N]^+OH^- \rightarrow (CH_3CH_2CH_2)_3N + C_3H_6 + H_2O\ (523\ K)$$

$$[(CH_3CH_2CH_2)_4N]^+F^- \rightarrow (CH_3CH_2CH_2)_3N + C_3H_6 + HF\ (548\ K)$$

$$(CH_3CH_2CH_2)_3N \rightarrow (CH_3CH_2CH_2)_2NH + C_3H_6\ (548-723\ K)$$

$$(CH_3CH_2CH_2)_2NH \rightarrow (CH_3CH_2CH_2)NH_2 + C_3H_6$$

$$(CH_3CH_2CH_2)NH_2 \rightarrow NH_3\uparrow + C_3H_6$$

To study the carbonization process of the TPAOH molecules in the $AlPO_4$-5 crystal channels, we measured the Raman spectra of TPAOH−$AlPO_4$-5 crystals during the pyrolysis process (in the temperature range 300−823 K). The result is shown in Figure 7a. At room temperature, the curve shows typical characteristic Raman-active modes for TPAOH molecules. The peak near 1036−1150 cm^{-1} is attributed to the C−N stretching vibration mode. The peak at ∼1458 cm^{-1} is assigned to the CH_3 antisymmetrical deformation mode, and the peaks near 2887−3050 cm^{-1} are due to the C−H bond-stretching modes.[25] When the $AlPO_4$-5 crystals were pyrolyzed at the temperature of 573 K, the C−H stretching modes in the region 2850−3050 cm^{-1} remained essentially the same as that at 373 K, except that the intensities decreased. The decrease in the relative intensities at 940 cm^{-1} (due to the C−N vibration) and 1040 and 1460 cm^{-1} (due to CH_3) indicates that low alkylated amines (dipropylamine and *n*-propylamine) were formed. The *G*-like bands near 1600 cm^{-1} and the disorder-induced *D* band appeared when the sample was heated to above 698 K. At even higher temperatures, the intensity of the *G*-like bands was gradually enhanced. The sharpness of the peaks is an indicator that carbon atoms were graphitized in the channels. As a result, the color of the crystal changed from transparent to black with a significant amount of optical anisotropy. The radial breathing mode (RBM) bands at 510 and 550 cm^{-1}, indicative of the 4 Å carbon nanotubes, appeared at ∼723 K, with their relative intensity increasing with increasing temperature. Figure 7b shows the Raman spectrum of 0.4 nm SWNTs inside the channels of $AlPO_4$-5. As a reference, the Raman spectrum of calcined $AlPO_4$-5 single crystal is shown as well. Because of the resonance enhancement, the Raman intensity of SWNTs is at least 20 times stronger than that of $AlPO_4$-5. Thus the contribution of the vibrations from the $AlPO_4$-5 framework to the Raman spectra is negligible. In particular, there also exist complex Raman signals for the $AlPO_4$-5 framework at frequencies 398−500 cm^{-1} (as shown in the inset of Figure 7), arising from the deformations of four T-atom-membered rings.[26] The RBMs at 510 and 550 cm^{-1}, which are clearly absent in the calcined crystal, accompanied by the G lines at 1600 cm^{-1}, confirm that a carbon tubular structure has been formed. We also observed the RBM of free-standing SWNTs after removing the zeolite framework.[27]

The decomposition of TPAOH molecules results in the successive release of propylene molecules. These C_6H_6 can be either pyrolyzed into smaller molecules (such as CH_4 and C_2H_4) and subsequently carbonized in the channels or converted into bigger molecules such as 2-methyl-butane and xylene. The number of carbon atoms that can be kept inside the channels is determined by the competition between these two processes, i.e., of carbonization and conversion. The $AlPO_4$-5 crystals can substitute other metal cations into their frame structure, giving rise to the formation of surface acidity. The dependence of the catalytic effect and selectivity on surface acidity in the transformation process of the carbon precursor into 0.4 nm SWNTs inside the crystals channels can be very different for different metal-cation substitutions. Details will be given elsewhere.

4. Concluding Remarks

We have fabricated 0.4 nm SWNTs inside the channels of $AlPO_4$-5 single crystals by pyrolyzing four different carbon precursor molecules and investigated their effect(s) on the formation of SWNTs. The quality and filling density of the SWNTs improved with an increase in the carbon source density, and the TPAOH is found to be the best for carbon nanotubes synthesis. The TPAOH molecules decompose into lighter amines with the abstraction of propylene and the stepwise formation of tripropylamine, dipropylamine, and *n*-propylamine. The 0.4 nm nanotubes are formed at about 723 K.

(25) During, H. R.; Beshir, W. B.; Gogley, S. E.; Hizer, T. J. *J. Raman Spectrosc*. **1989**, *20*, 311.
(26) Hollmes, A. J.; Kirkby, S. J.; Ozin, G. A.; Young, D. *J. Phys. Chem*. **1994**, *98*, 4677.
(27) Ye, J. T.; Tang, Z. K. *Phys. Rev. B*. **2005**, *72*, 045414.

Acknowledgment. The authors are grateful to Dr. B. R. Shi at MCPF of HKUST and Dr. Frank Lam in the Department of Chemical Engineering. This research was supported by Hong Kong RGC Grants 605003, HKUST6057/02P, HKUST6149/01P, RGC DAG04/05.SC24, and RGC Central Allocation CA04/05.SC02. I.L.L. thanks Shenzhen STI (200432) and Guangdong Natural Science Foundation (5301084) for financial support.

CM0526821